Inorganic Chemistry

ARTICLE

pubs.acs.org/IC

Cobalt Cystathionine β-Synthase: A Cobalt-Substituted Heme Protein with a Unique Thiolate Ligation Motif

Aaron T. Smith,[†] Tomas Majtan,[‡,§] Katherine M. Freeman,[†] Yang Su,[†] Jan P. Kraus,[‡] and Judith N. Burstyn*[,†]

[†]Department of Chemistry, University of Wisconsin—Madison, 1101 University Ave., Madison, Wisconsin, 53706, United States

[‡]Department of Pediatrics, University of Colorado Denver, Aurora, Colorado 80045, United States

[§]Department of Genomics & Biotechnology, Institute of Molecular Biology SAS, Dubravska cesta 21, Bratislava, 84551, Slovakia

Supporting Information

ABSTRACT: Human cystathionine β-synthase (hCBS), a key enzyme in the trans-sulfuration pathway, catalyzes the condensation of serine with homocysteine to produce cystathionine. CBS from higher organisms is the only known protein that binds pyridoxal-5′-phosphate (PLP) and heme. Intriguingly, the function of the heme in hCBS has yet to be elucidated. Herein, we describe the characterization of a cobalt-substituted variant of hCBS (Co hCBS) in which CoPPIX replaces FePPIX (heme). Co(III) hCBS is a unique Co-substituted heme protein: the Co(III) ion is 6-coordinate, low-spin, diamagnetic, and bears a cysteine(thiolate) as one of its axial ligands. The peak positions and intensities of the electronic absorption and MCD spectra of Co(III) hCBS are distinct from those of previously Co-substituted heme proteins; TD-DFT calculations reveal that the unique features arise from the 6-coordinate Co bound axially by cysteine(thiolate) and a neutral donor, presumably histidine. Reactivity of Co(III) hCBS with $HgCl_2$ is consistent with a loss of the cysteine(thiolate) ligand. Co(III) hCBS is slowly reduced to Co(II) hCBS, which contains a 5-coordinate, low-spin, $S = 1/2$ Co-porphyrin that does not retain the cysteine(thiolate) ligand; this form of Co(II) hCBS binds $NO_{(g)}$ but not $CO_{(g)}$. Co(II) hCBS is reoxidized in the air to form a new Co(III) form, which does not contain a cysteine(thiolate) ligand. Canonical and alternative CBS assays suggest that maintaining the native heme ligation motif of wild-type Fe hCBS (Cys/His) is essential in maintaining maximal activity in Co hCBS. Correlation between the coordination structures and enzyme activity in both native Fe and Co-substituted proteins implicates a structural role for the heme in CBS.

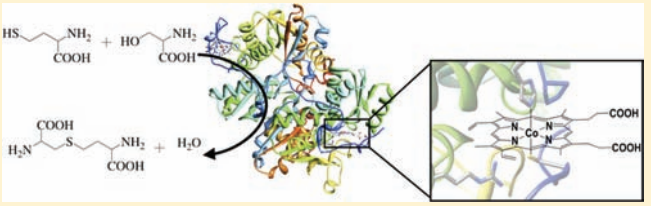

INTRODUCTION

Cystathionine β-synthase (CBS) is a pyridoxal-5′-phosphate (PLP)-dependent enzyme that lies at a critical branch point in the methionine metabolic cycle. CBS is chiefly responsible for the condensation of homocysteine, a toxic metabolite and byproduct of sulfur metabolism, with serine to form cystathionine.[1] Mutations in the gene that codes for human CBS allow for the accumulation of plasma homocysteine, resulting in a condition called CBS-deficient homocystinuria (CBSDH). This condition is manifested physiologically by a variety of symptoms, ranging from vascular occlusions to dislocated ocular lenses, skeletal problems, and mental retardation as well as an increased risk of Alzheimer's and Parkinson's diseases.[2−5]

Mammalian CBS is unique in that it is the only known PLP-dependent enzyme to also contain a heme *b* cofactor, and since the heme is proposed to function as a regulatory site, the relationship between these cofactors is of interest. CBS exists as an α_4 homotetramer of 63-kDa subunits. Each enzyme subunit contains three domains: N-terminal, central catalytic, and C-terminal; these domains bind heme, PLP, and S-adenosylmethionine (AdoMet), respectively.[6,7] Binding of AdoMet to the C-terminal domain functions in allosteric regulation by increasing enzyme activity approximately 4-fold.[8] Removal of the C-terminal domain results in a truncated, 45-kDa form of CBS (CBS-45) in which the oligomeric status of the enzyme has changed from a tetramer to a dimer. Truncation is accompanied by a loss of responsiveness to AdoMet and an approximate 3-fold increase in activity. CBS-45 has been successfully crystallized and used to elucidate the tertiary structure of the enzyme and the ligands to the heme cofactor. The heme is located in proximity to the PLP active site, with the closest edge of the heme macrocycle positioned approximately 14 Å from the PLP phosphate.[9−11]

The heme of CBS is axially coordinated via an uncommon Cys/His motif that involves the thiolate of Cys^{52} trans to the $N_{\varepsilon 2}$ atom of His^{65} with the amino acid ligands both provided by the N-terminal tail of the polypeptide.[10,12] While the catalytic condensation reaction of homocysteine and serine can be fully explained by reaction at the PLP cofactor, heme is necessary for optimal activity.[6,13−16] CBS from lower organisms such as *Saccharomyces cerevisae* and *Trypanosoma cruzi* lack the N-terminal motif or the C- and N-terminal motifs, respectively, that bind

Received: December 30, 2010
Published: April 11, 2011

AdoMet and heme, making them unresponsive to the allosteric regulator and exogenous forms of the cofactor; these observations suggest that AdoMet and heme are recent evolutionary acquisitions.[17−19] The heme of CBS was initially postulated to function as a redox sensor, based on decreased enzymatic activity in the ferrous form. The logic behind such redox regulation would be to control the flux between the trans-sulfuration (utilizing CBS) and transmethylation (utilizing methionine synthase) pathways.[11,20,21] Yet, it has been shown that activity of the ferrous and ferric forms of CBS are identical when Cys^{52} is retained and that the decrease in activity upon reduction is likely due to an irreversible ligand switch at the heme.[22−24] In all cases studied to date where the heme Fe−Cys^{52} bond was disrupted or modified, including reactions with NO, CO, $HgCl_2$, and peroxynitrite, enzyme activity was lost.[22,25−28] The link between this loss of activity *in vitro* and CBS heme function *in vivo* is uncertain; consequently, the role of the heme in CBS is still unknown.

We report herein characterization of a cobalt-substituted variant of human CBS (Co hCBS). Recently, we described the expression of Co hCBS in *E. coli* and its purification to homogeneity.[29,30] In this study, we demonstrate that the as-isolated form of Co hCBS is in the Co(III) oxidation state, is active in both the canonical assay and an alternative CBS reaction assay, and bears a Cys/His Co(III) porphyrin ligation motif similar to that of WT Fe(III) hCBS but unprecedented in cobalt porphyrin-substituted proteins. We show that cysteine ligation to the Co(III) porphyrin may be disrupted upon reaction of the enzyme with $HgCl_2$, and that this metal−thiolate bond disruption occurs with a concomitant reduction in enzyme activity. We also demonstrate that the Co-substituted enzyme can access the Co(II) oxidation state, likely forming a 5-coordinate, His-ligated Co(II) porphyrin, which will bind $NO_{(g)}$ but not $CO_{(g)}$. Formation of the 5-coordinate Co(II) porphyrin with a concomitant loss of the cysteine(thiolate) ligand correlates with a significant loss in enzymatic activity. On the basis of these findings, we postulate that the Co porphyrin binds to hCBS similarly to how it does to heme in the WT enzyme, and that the enzyme is unable to distinguish between heme (FePPIX) and CoPPIX. These data are consistent with a structural role for the CBS heme, where this structural component modulates enzyme activity.

MATERIALS AND METHODS

Materials. Materials used in buffer preparation were purchased from Sigma-Aldrich and used as received. $NO_{(g)}$ was generated *in situ* by mixing $NaNO_2$ (Sigma-Aldrich), $CuCl_2$ (MCB Chemicals), and *L*-ascorbic acid (99+%, Sigma-Aldrich) with a previously prepared buffer solution. Appropriate imidazole solutions were made with 1-methylimidazole (99%, redistilled) or 4-methylimidazole (99%) both from Sigma-Aldrich. Co(III)PPIX-Cl was purchased from Frontier Scientific, Inc. and stored in a desiccator until used. $HgCl_2$ solutions were made fresh for each experiment from solid $HgCl_2$ (J.T. Baker, Inc.). Ninhydrin was purchased from Fluka; ninhydrin reagent was prepared by dissolving 0.25 g of ninhydrin (as received) in a mixture of 4 mL of concentrated HCl and 6 mL of concentrated acetic acid.

Isolation and Purification of Co hCBS. The expression and purification of human CBS containing CoPPIX was performed as described in our previous work.[24,29,30] Briefly, *E. coli* Rosetta2 (DE3) cells carrying the expression plasmid for WT human CBS (pGEX-6P1-hCBS WT) were grown overnight 12-times in M9 minimal medium supplemented with $CoCl_2$ (∼150 μM final concentration). The last culture served as an inoculum for large-scale expression and purification. Purification of Co hCBS essentially continued as described for WT hCBS[24,31] with the modifications described by Majtan et al.[29] Briefly, the CBS-GST fusion protein was isolated on GSH-Sepharose, and the GST fusion partner was cleaved with PreScission protease.[24] CBS was separated from GST by DEAE Sepharose chromatography.[29] The cobalt content in the final, purified Co hCBS was >90%.[29]

Electronic Absorption Spectroscopy. Electronic absorption spectra were recorded on a double-beam Varian Cary 4 Bio spectrophotometer with a temperature controller, set to a spectral bandwidth of 0.5 nm. Spectra were obtained at varying temperatures from 4 to 37 °C for samples of protein in 500 mM CHES with 100 mM NaCl, pH 9.0, as indicated. This nonphysiological pH was chosen because WT Fe hCBS is maximally active between pH 8.5 and 9.0, and natively coordinated (His^{65}/Cys^{52}) Fe(II)CBS is most stable at this pH.[20,32] For the $HgCl_2$ reaction, fresh stock $HgCl_2$ solutions were prepared for each experiment. The stock solution (∼ 60 mM, 10 μL) was administered at room temperature to achieve a final $HgCl_2$ concentration of 1−2 mM, and spectra were collected for ∼2 h or until no more spectral changes were observed. Reduction of Co(III) protein samples was accomplished by adding an anaerobically prepared stock solution of sodium dithionite or dithiothreitol (DTT), to achieve a final sample concentration of 1−5 mM. Samples were purged of oxygen by flowing $Ar_{(g)}$ through the headspace of a septum-sealed cuvette for ∼10 min. The solutions of dithionite or DTT and Co(III) protein were allowed to equilibrate at 4 °C before anaerobic addition of a stock reductant (∼30 mM, 10 μL) to the Co(III) protein. The temperature controller of the spectrophotometer was slowly raised to 37 °C, and the reduction of Co(III) to Co(II) was monitored over ∼1 h or until no further spectral changes were observed. Spectra of reduced Co(II) hCBS are reported for reduction with DTT. Analysis by MCD and EPR spectroscopies indicated the formation of a diamagnetic Co(II) species upon dithionite reduction, possibly suggesting the formation of a $SO_2^{-\bullet}$−Co(II) adduct. NO adducts were prepared by injecting three 100 μL samples of $NO_{(g)}$ (generated by mixing $NaNO_2$, $CuCl_2$, *L*-ascorbic acid, and 1 mL of CHES stock buffer solution) to the headspace of a septum-sealed vial containing the Co(III) form of the protein. Reduction and binding of $NO_{(g)}$ were subsequently induced by anaerobic addition of a stock solution of DTT (∼30 mM, 10 μL), and the reaction was followed spectrophotometrically at 37 °C until no further changes were observed. Reoxidation of the Co(II) form of the protein was followed spectrophotometrically over the course of 2 days by introducing ambient air to the septum-sealed cuvette containing the DTT-reduced protein. Co(III)PPIX-Cl standards were made by dissolving the solid in either CH_2Cl_2 or 1:100 (v/v) DMSO/H_2O, with ∼0.5 mL of 6M NaOH per every 100 mL. Porphyrin concentrations were determined using ICP-OES, to give the metal concentration, and Beer's law using the appropriate ε value. Imidazole solutions (4-MeImH or 1-MeIm) were prepared in either CH_2Cl_2 or 1:100 (v/v) DMSO/H_2O, and 1 or 2 equivalents were added to the Co(III) porphyrin solution in septum-sealed cuvettes. Ligand binding was monitored spectrophotometrically.

MCD Spectroscopy. Magnetic circular dichroism (MCD) spectra were recorded on a Jasco J-715 CD spectropolarimeter with the sample compartment modified to accommodate an SM-4000-8T magnetocryostat (Oxford Instruments). The buffer used for the MCD samples was 500 mM CHES, 100 mM NaCl, pH 9.0, with approximately 55% (v/v) glycerol present in the final sample. Glycerol was introduced to the Co(III) form of the protein and stirred with a syringe until the solution was homogeneous. Co(II) samples were prepared from glycerol-containing Co(III) protein solutions, with monitoring of the visible spectral changes at 37 °C. The final concentrations were DTT, ∼5 mM; protein, ∼30 μM in a total volume of 125 μL. Glycerol had no effect on the electronic absorption spectra at room or liquid-helium temperatures, for either Co(II) or Co(III) hCBS. Samples were transferred via gastight

syringe into cells purged with $Ar_{(g)}$, flash-frozen, and stored in $N_{2(l)}$. MCD spectra were taken over a temperature range from 4 to 200K. The MCD signal at each temperature was recorded at ±7 T. Negative polarity data were subtracted from positive polarity data to remove CD contributions, and the resulting spectrum was divided by 2. For the spectra of Co(III) and Co(II) hCBS at 4 K, MCD contributions from the native Fe-containing enzyme (<8%) were subtracted from the Co hCBS signal. The resulting difference spectrum was compared to the high-temperature spectrum (50 K), in which the paramagnetic signals were minimized. These spectra were virtually indistinguishable.

EPR Spectroscopy. X-band electron paramagnetic resonance (EPR) spectra were collected on a Bruker ESP 300E equipped with an Oxford ESR 900 continuous flow cryostat connected to an Oxford ITC4 temperature controller. The microwave frequency was monitored using an EIP model 625A CW microwave frequency counter. Field calibration was achieved using a Varian ER 035 M gaussmeter. Spectra of Co(II) hCBS and of Co(II)PPIX model complexes were recorded in a 500 mM CHES buffer and 100 mM NaCl at pH 9.0. Co(II) protein samples were prepared from Co(III) protein solutions in a buffer, with monitoring of the visible spectral changes at 37 °C. The final concentrations were: DTT, ~16 mM; protein, ~150 μM in a total volume of 200 μL. Co(II)PPIX model complex solutions were prepared from Co(III)PPIX model complex solutions in glycerol and a buffer, with monitoring of the visible spectral changes at 37 °C. The final concentrations were DTT, ~20 mM; Co(II)PPIX complex, ~200−400 μM in a total volume of 1000 μL and 55% glycerol (v/v). Each sample was transferred via a gastight syringe into an $Ar_{(g)}$-filled quartz EPR tube and frozen in $N_{2(l)}$. For all samples, scans of 0−10 000 G revealed no signals other than those reported. EPR data were simulated using the WEPR program written by Neese.[33]

Computations. All calculations were performed on a Dell Vostro desktop PC. Initial geometric models for Co(III)(porphine)-(4-MeImH)thiophenolate [Co(P)(4-MeImH)(SPh)] and Co(III)-(porphine)(4-MeImH)methanethiolate [Co(P)(4-MeImH)(SMe)] were based on the optimized coordinates of computational models of analogous iron(III) five-coordinate, high-spin, thiolate-bound heme systems to which 4-methylimidazole was added as a sixth ligand.[34,35] Spin-restricted (S = 0) geometry optimizations of each cobalt model were performed using ORCA 2.6.35 software developed by Dr. Frank Neese (MPI Mülheim, Mülheim, Germany) implementing the B3LYP correlation functional.[36,37] A triple-ζ Slater-type orbital (STO) basis set, with the Ahlrichs polarized split valence basis SV(P) and SV/C auxiliary basis sets, was chosen for all atoms except Co and S, to which an additional polarization function (TZVP) was applied. Core orbitals were frozen through 1s for C and N and through 2p for Co and S. Time-dependent density-functional theory (TD-DFT) calculations were performed similarly using ORCA 2.6.35 and the same basis sets and functionals. A total of 40 excited states were calculated within a range of ±3 hartree from the highest occupied molecular to the lowest unoccupied molecular orbital gap. Isosurface plots of relevant molecular orbitals and electron density difference maps were generated with Laaksonen's gOpenMol program, v. 3.00.[38,39]

CBS Activity Assays. The activities of Co(III) hCBS, Hg-reacted Co(III) hCBS, and Co(II) hCBS were measured in the canonical cystathionine synthesis reaction[29] and one alternative cysteine synthesis reaction. To monitor cysteine synthesis, the reaction mixture (600 μL) contained 0.5 mg/mL BSA, 10 mM DTT, 0.5 mM PLP, 0.36 mM AdoMet, 0.015 mg/mL enzyme, 24 mM L-serine, and 25.5 mM Na_2S in 200 mM Tris buffer (pH 8.6). The reaction temperature was maintained at 37 °C; the total incubation time was 12 min, with measurements at 4, 6, 8, 10, and 12 min. The cysteine concentration at each of the five time points was measured using a colorimetric method.[40] A sample (100 μL) of the reaction mixture was taken and mixed with 50% (w/v) trichloroacetic acid (20 μL). The precipitated protein was removed by centrifugation. The supernatant (100 μL) was combined with acetic acid (100 μL) and ninhydrin reagent (100 μL); the mixture was heated in a boiling water bath for 3 min and immediately cooled in ice water. The absorbance at 560 nm was measured to determine the amount of cysteine produced. A standard curve was generated by the same method using cysteine solutions of known concentration and containing all other reagents except the enzyme. To prepare Hg-reacted Fe(III) hCBS or Co(III) hCBS for assay, $HgCl_2$ was added as described (*vide supra*) and allowed to react for 2 h. The protein solution, containing excess $HgCl_2$, was loaded onto a YM-30 Amicon Ultra spin concentrator (Millipore) and washed three times by concentration and dilution into a fresh Tris buffer (200 mM, 100 mM NaCl, pH 8.6) using a table-top centrifuge (RCF 15 000*g*). Hg-treated Fe(III) hCBS or Co(III) hCBS was diluted in the final step to achieve a protein concentration of ~0.7 mg/mL. To prepare Co(II) hCBS for assay, Co(III)hCBS was preincubated with 10 mM DTT, 0.5 mg/mL BSA, and 0.5 mM PLP at 37 °C for 3 h. For enzymatic reactions catalyzed by Fe(III) and Co(III) hCBS, Hg-reacted or not, the reaction was initiated by adding the enzyme. For reactions catalyzed by Co(II) hCBS, the reaction was initiated by adding the substrates.

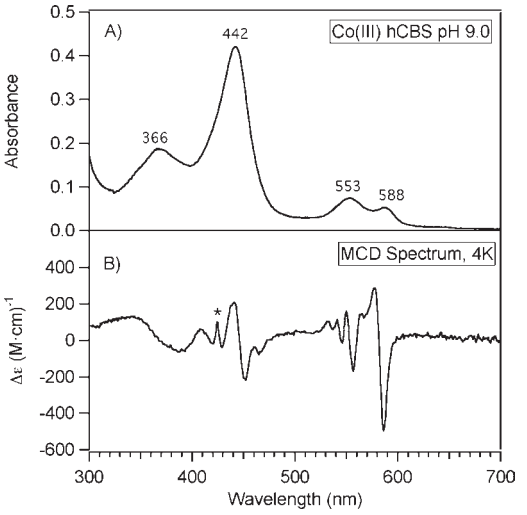

Figure 1. (A) Electronic absorption spectrum of Co(III) hCBS. Co(III) hCBS (3.9 μM) was in 500 mM CHES buffer and 100 mM NaCl at pH 9.0 and room temperature. (B) MCD spectrum of Co(III) hCBS. Protein concentration was 31.1 μM in 225 mM CHES buffer, 45 mM NaCl, and 55% glycerol (v/v) at 4 K and 7 T, with the residual Fe(III) hCBS signal subtracted. The asterisk (*) indicates the presence of a residual overlapping, paramagnetic Fe(III) signal unable to be removed without significantly altering the spectral integrity.

RESULTS

Co(III) hCBS Displays Unique Spectral Properties. The electronic absorption features of Co(III) hCBS are unique among the family of Co-substituted heme proteins. The band shapes and positions of this spectrum, shown in Figure 1A, are characteristic of the Co(III) oxidation state.[41,42] Notable are the distinct α and β bands (588 and 553 nm, respectively) and a sharp Soret peak (442 nm); identical spectra were observed for Co(III) hCBS at pH 7.4 (500 mM HEPES, 100 mM NaCl) and at pH 6.0 (500 mM MES, 100 mM NaCl; data not shown). A comparison of Co(III) hCBS to other Co-substituted proteins (Table 1) reveals that the electronic absorption spectrum of Co(III) hCBS is distinct. All three absorption bands of Co(III) hCBS are red-shifted relative to those of Co(III)-Hb, Mb, HRP,

dx.doi.org/10.1021/ic102586b |*Inorg. Chem.* 2011, 50, 4417–4427

Table 1. Comparison of Co(III) hCBS Electronic Absorption Peak Positions (nm) with Those of Other Select Co-Substituted Proteins and Co(III) PPIX Models[a]

Co(III) species	δ	Soret (γ)	β	α	ligands	spin state	ref.
Co hCBS pH 9.0	366	442	553	588			this work
Co hCBS pH 9.0 + $HgCl_2$	~ 350	427	538	573			this work
Co $hCBS_{Reox}$	~ 351	424	538	569			this work
$CoPPIX(4\text{-MeImH})_2$	352	426	542	573	4-MeImH/4-MeImH	LS	this work
$CoPPIX(1\text{-MeIm})_2$	354	423	535	568	1-MeIm/1-MeIm	LS	this work
Co Hb[b]	NR[b]	433	535	568	His/His	LS	50, 51
Co Hb (O_2^-)[c]	NR[b]	428	538	571	His/O_2^-	LS	50, 51
Co Mb (O_2^-)[c]	NR[b]	426	539	577	His/O_2^-	LS	50, 51
Co HRP (pH > 9.5)	NR[b]	427	533	565	His/H_2O	LS	52
Co Cyt *c*	NR[b]	426	530	567	His/Met	LS	41, 61
CoPPIX(TGE)(ImH)	356	430	548	576	RS^-/ImH	LS	62
CoPPIX(TGE)(1-MeIm)	357	430	547	576	RS^-/1-MeIm	LS	62
CoPPIX(TGE)(2-MeIm)	370	435	562	576	RS^-/2-MeImH	LS	62
CoPPIX(TGE)(4-MeIm)	360	431	548	575	RS^-/4-MeImH	LS	62
CoPPIX(TN)(ImH)	358	430	546	575	RS^-/ImH	LS	62
$CoPPIX(TGE)_2$	372	465		574	RS^-/RS^-	LS	62
$CoPPIX(TGB)_2$	373	464		574	RS^-/RS^-	LS	62
$CoPPIX(TGEH)_2$	373	463		575	RS^-/RS^-	LS	62
$CoPPIX(TN)_2$	370	463		572	RS^-/RS^-	LS	62
Co P-450_{cam}(DTT)	375	467		573	RS^-/RS^-	LS	43

[a] TGE = thioglycolate ethyl ester; TN = thionalide; TGB = thioglycolate *n*-butyl ester; TGEH = thioglycolate 2-ethylhexyl ester.[b] Not reported. [b] Met form; i.e., Co(III) Hb bearing two His residues. [c] Oxy form; i.e., Co(III) Hb/Mb superoxide adduct.

and Cyt *c*, which are 6-coordinate with neutral or weakly donating anionic ligands. These red shifts suggest that at least one strongly electron-donating ligand is bound to the Co(III) center; however, the red shifts of the Co(III) hCBS spectrum are not as pronounced as those of the dithiolate-coordinated Co(III) $P450_{cam}$(DTT).[43] Furthermore, Co(III) hCBS exhibits distinct α and β bands, in contrast to the poorly resolved absorption envelope of Co(III) $P450_{cam}$(DTT). These observations suggest that the axial ligands surrounding the cobalt center in Co(III) hCBS are different from those of other previously observed cobalt-substituted heme proteins.

Co(III) porphyrin model compounds provide insight into the nature of the unusual coordination environment in Co(III) hCBS. The Co(III) hCBS spectrum is different from those of 6-coordinate Co(III) PPIX complexes with bis-imidazole or bis-thiolate; however, there is a reasonably close match between the Co(III) hCBS spectrum and those of Co(III) PPIX complexes with one imidazole and one thiolate ligand (Table 1). These imidazole-thiolate-bound model compounds exhibit red-shifted peak maxima, with distinct α and β bands, albeit at slightly higher energy than those of Co(III) hCBS. A further important similarity is the presence of a relatively intense δ band, which is characteristic of a thiolate-to-metal charge transfer transition mixing with the porphyrin $\pi \rightarrow \pi^*$ transition. Overall, there exists a distinct correlation between the red shifts of the electronic absorption spectrum and the number of thiolate ligands bound to the Co(III) center. These comparisons suggest that the coordination environment in Co(III) hCBS is like that of Fe(III) hCBS, with one thiolate and one histidine as the axial ligands.

Co(III) hCBS was further characterized by MCD spectroscopy (Figure 1B) to isolate the Co(III) porphyrin spectral contributions from that of the native Fe(III) heme, and to confirm that the Co coordination environment is distinct from those of previously studied Co-substituted heme proteins. Co(III) hCBS was previously shown to contain a majority of Co (92%) and a residual amount of Fe (~8%).[29] Co(III) porphyrins are consistently low-spin;[42,43] because of this property, the MCD signature of a Co(III) porphyrin-containing protein should show no temperature dependence, indicative of the cobalt's d^6, $S = 0$ ground state.[44] At 4 K, Co(III) hCBS exhibits signals that reflect contribution from both Co(III) and Fe(III), consistent with metal analyses that show ~8% Fe in the Co hCBS protein.[29] Paramagnetic low-spin Fe(III) gives temperature dependent MCD spectra. At 50 K, the Fe(III) contribution to the MCD spectrum is minimized, and the signature of diamagnetic low-spin Co(III) hCBS dominates. Figure 1B shows the 4 K MCD spectrum of Co(III) hCBS from which the contribution of the Fe(III) was removed by subtraction. This spectrum is virtually identical to that obtained at 50 K. No temperature dependence of the Co(III) signal is observed, consistent with the predicted spin state. The isolated spectral MCD signatures of Co(III) hCBS are shown in Table 2 and compared with that of the native Fe(III) hCBS. As is typical with many diamagnetic d^6 metal porphyrins, the temperature-independent, derivative-type *A* terms in the α−β region of the spectrum dominate in intensity when

Table 2. Comparison of MCD peak, crossover, and trough positions (nm) between Co(III) hCBS and Fe(III) hCBS.[32]

	band	peak	crossover	trough
Co(III) hCBS	Soret (γ)	442	446	452
	β	551	553	557
	α	577	582	587
Fe(III) hCBS	Soret (γ)	419	425	433
	α/β	545	555	567

dx.doi.org/10.1021/ic102586b |*Inorg. Chem.* 2011, 50, 4417–4427

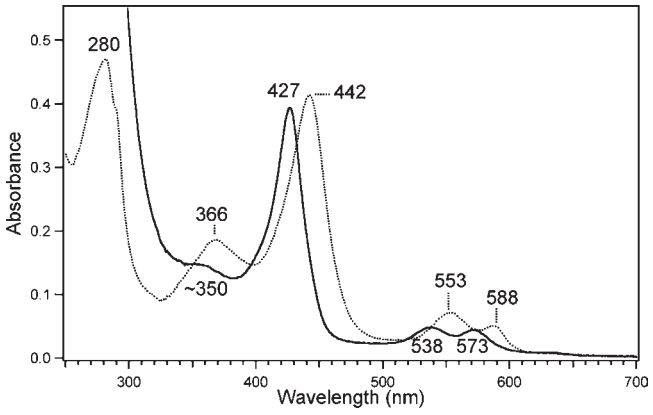

Figure 2. Electronic absorption spectra of Co(III) hCBS before (····) and 2 h after (—) addition of $HgCl_2$. Co(III) hCBS (3.9 μM) was in a 500 mM CHES buffer and 100 mM NaCl at pH 9.0 with $HgCl_2$ added to a final concentration of 1.26 mM.

compared to the *A* term in the Soret region.[45,46] In the MCD spectrum of the Co(III) protein, the shape of the term resulting from the $\pi \rightarrow \pi^*$ transition of the Soret region is similar to that of other Co(III) porphyrins.[47] The $\alpha-\beta$ MCD transitions lie on the red edge of the absorption maxima, and the *A* terms display moderate asymmetry with multiple crossover peaks. These observations implicate charge-transfer bands that overlap in this region.[47] These characteristics are not observed in the MCD spectrum of a model compound Co(III)PPIX(1-MeIm)$_2$ (Supporting Information Figure S1), implying that the coordination environment of Co(III) hCBS does not contain two neutral donor ligands.

Co(III) hCBS Has One Axial Thiolate Ligand. The reactivity of Co(III) hCBS confirms the presence of a thiolate ligand. $HgCl_2$, a known metal−thiolate bond disrupter,[27,48,49] reacts with Co(III) hCBS, as shown in Figure 2. Immediately upon the addition of $HgCl_2$, changes were evident in the electronic absorption spectrum. The Soret and $\alpha-\beta$ bands immediately broadened and blue-shifted; the δ band, normally intense in thiolate-ligated metalloporphyrins due to orbital mixing between the sulfur and the metal, became nondescript and indistinct. After 2 h, the spectrum had settled into a new position with peak maxima at 427 nm (Soret), 538 nm (β), and 573 nm (α). These spectral changes are evidence that $HgCl_2$ disrupted a Co(III)−thiolate bond. The final spectrum was consistent with that of a Co(III) porphyrin bearing two neutral donor ligands, as revealed by the comparison of peak positions for the Hg-disrupted Co(III) hCBS protein with those of other Co-substituted proteins and model compounds (Table 1). This comparison clearly shows that when the thiolate ligand is lost, the Co(III) hCBS protein compensates by providing an alternate neutral ligand. The addition of β-mercaptoethanol to the Hg-disrupted Co(III) hCBS protein did not result in further spectral changes (data not shown). Thus, β-mercaptoethanol was unable to reverse the Hg-induced ligand switch, in contrast to some other heme-thiolate proteins.[48] The lengthy time for full conversion from thiolate-ligated Co(III) hCBS to the final Hg-disrupted form, and the fact that this process does not proceed with isosbestic spectral conversion, suggests that Co−thiolate bond disruption occurs faster than replacement with the alternate neutral donor ligand. However, no discrete spectrum for a 5-coordinate intermediate was observed.

Time-dependent density-functional theory (TD-DFT) calculations support the presence of a thiolate ligand bound to Co(III) hCBS. Calculations were carried out on two closed shell $S = 0$ cobalt model compounds (Figure 3): Co(III)(porphine)(4-MeImH)thiophenolate [Co(P)(4-MeImH)(SPh)] and Co(III)-(porphine)(4-MeImH)methanethiolate [Co(P)(4-MeImH)-(SMe)]. Geometry-optimized structures were calculated, and these structures served as the input for time-dependent calculation of electronic absorption spectra. The predicted absorption spectra exhibit two dominant transitions (γ, δ) of comparable intensity, with the lower energy transition (γ) arising from pure porphyrin $\pi \rightarrow \pi^*$ transfer transitions, and the higher energy transition (δ) arising from the mixing of porphyrin $\pi \rightarrow \pi^*$ and ligand-to-metal charge transfer (LMCT) (S(p) $\rightarrow$ Co(d_σ)) transitions. Figure 3C illustrates the select charge-transfer transition that mixes with the porphyrin $\pi \rightarrow \pi^*$ transfer transitions (not shown) and gives rise to the intense δ band. The dark blue color on the sulfur(thiolate) p orbital represents loss of electron density; the light green color on the cobalt d orbital represents a gain of electron density. Thus, the presence of an intense δ band arises from the unique donor character of a single thiolate ligand. Additional charge transfer bands are predicted to occur at wavelengths beyond the $\alpha-\beta$ region; however, the predicted intensity of these transitions is extremely weak. The prediction of a prominent δ band by calculation correlates well with the observation of such a δ band in the electronic absorption spectrum of Co(III) hCBS, corroborating the presence of a thiolate ligand bound to the Co(III) center.

Co(II) hCBS Is Similar to Other Known Co-Substituted Heme Proteins. Two redox states of Co hCBS, Co(III) and Co(II), are accessible, as is typical of other Co porphyrin-substituted heme proteins.[41,50−53] Figure 4 depicts the conversion from Co(III) hCBS to Co(II) hCBS, induced by addition of a DTT solution at a pH of 9.0. Reduction is slow, requiring approximately 3.5 h to complete the reaction at 37 °C (Figure 4, inset). Interestingly, this reduction is strongly pH dependent, proceeding slowly at pH 9.0 and pH 6.0 at 37 °C, and exceedingly slowly at pH 7.4 at 37 °C. Under these physiological conditions, reduction was not complete after 8 h. A pH dependence on the rate of reduction of Co porphyrin-substituted heme proteins has been observed previously.[41] The reduction rate of Co(III) hCBS was also temperature dependent. At <4 °C, no discernible reduction takes place; at >4 °C, Co hCBS exists as a mixture of oxidation states until it is fully reduced at a high temperature (37 °C) and a high pH (9.0). Once fully reduced, cooling the protein does not reverse the reduction process.

Co(II) hCBS (Figure 5A) appears to be 5-coordinate, most plausibly retaining a single histidine ligand. Table 3 compares the electronic absorption spectrum of Co(II) hCBS to those of other Co-substituted proteins. This comparison reveals that Co(II) hCBS resembles other 5-coordinate Co(II) proteins. When 6-coordinate Co porphyrin-substituted heme proteins are reduced, the loss of one axial ligand is observed. The ligand that is retained is typically histidine, which may be identified in EPR spectra by the presence of superhyperfine coupling between the unpaired electron ($S = 1/2$) and the imidazole nitrogen ($I = 1$) superimposed on the hyperfine coupling with the Co nucleus ($I = {}^7/_2$).[50−53] An exception is Co(II)-substituted $P450_{cam}$, in which the thiolate ligand is retained.[43] Co(III) hCBS bears both a histidine and a thiolate, and either is a candidate to be lost upon reduction. The similarity of the Co(II) hCBS electronic absorption spectrum to that of 5-coordinate histidine ligated Co

dx.doi.org/10.1021/ic102586b |*Inorg. Chem.* 2011, 50, 4417–4427

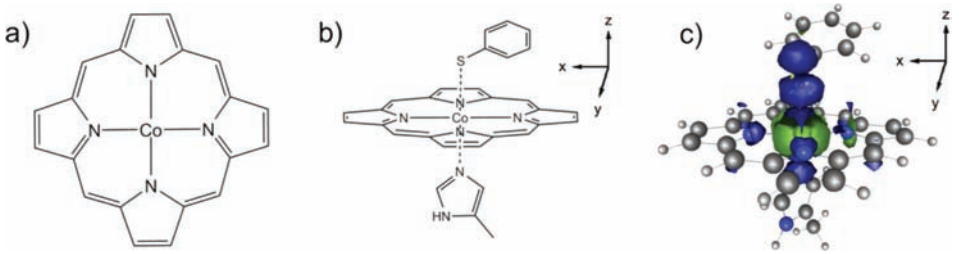

Figure 3. (A) Stick representation of Co(III) porphine [Co(III)P]. (B) Stick representation of Co(III)(porphine)(4-MeImH)(thiophenolate) [Co(P)(4-MeImH)(SPh)]. (C) TD-DFT computed electron density difference map (EDDM) of the selected transition that illustrates the ligand-to-metal charge transfer transition (LMCT, S(p) $\rightarrow$Co(d_σ)) in the model [Co(P)(4-MeImH)(SPh)]. Dark blue represents the loss of electron density; light green represents the gain in electron density.

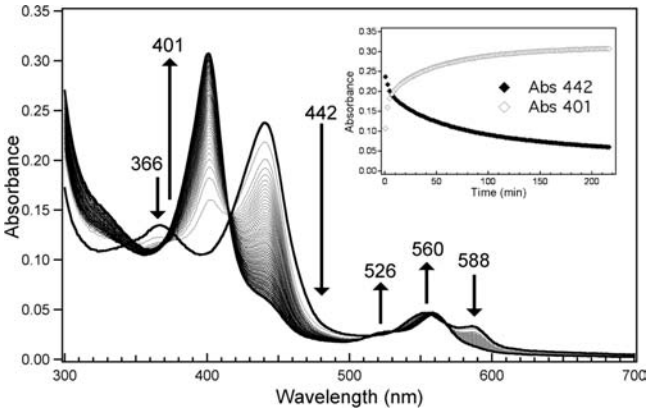

Figure 4. Electronic absorption spectrum of the reduction of Co(III) hCBS to Co(II) hCBS. Co(III) hCBS (3.9 μM) was in a 500 mM CHES buffer and 100 mM NaCl at pH 9.0 with 5.3 mM DTT (final concentration) at 37 °C. Inset: Time-dependent spectral change monitored at the noted wavelengths following the reduction of Co(III) hCBS (♦) to Co(II) hCBS (◊).

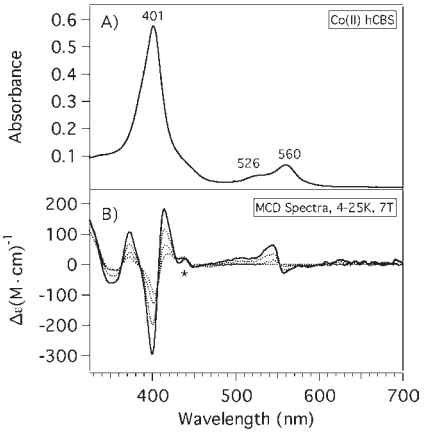

Figure 5. (A) Electronic absorption spectrum of Co(II) hCBS. Co(II) hCBS (3.9 μM) was in a 500 mM CHES buffer, 100 mM NaCl at pH 9.0, and 1.3 mM DTT (final concentration) at room temperature. (B) MCD spectra of Co(II) hCBS. Co(II) hCBS (31.1 μM) was in a 225 mM CHES buffer, 45 mM NaCl, 55% glycerol (v/v), and 24.7 mM DTT (final concentration) at 4−25 K and 7 T. An asterisk (∗) indicates the presence of an overlapping, diamagnetic Co(III) signal unable to be removed without significantly altering the spectral integrity.

proteins suggests that the thiolate is the ligand that is lost. Further support for this conclusion is drawn from the fact that the addition of $HgCl_2$ to the fully reduced Co(II) hCBS enzyme has no effect on the absorption spectrum (data not shown).

Table 3. Comparison of Co(II) hCBS Electronic Absorption Data (nm) with Other Select Co(II)-Substituted Proteins

Co(II) species	Soret (γ)	α/β	ligands	spin state	ref.
Co hCBS pH 9.0	401	560			this work
Co Hb	402	552	His (5c)	LS	50, 51
Co Mb	406	558	His (5c)	LS	50, 51
Co sGC	405	560	His (5c)	LS	53
Co HRP	401	553	His (5c)	LS	52
Co P-450$_{cam}$	404	556	RS^- (5c)	LS	43

MCD spectroscopy further supports the conclusion that the metal ion is fully reduced, and that the spectral signatures of Co(II) hCBS arise from the Co center. The MCD signature of Co(II) hCBS (Figure 5B, Table 4) is similar to those of other reported Co(II) porphyrin complexes.[45,47] The intensity of the asymmetric *C* term (crossover at 554 nm) that corresponds to the $\alpha-\beta$ region of the electronic absorption spectrum is smaller than that of the *C* term that corresponds to the Soret region of the electronic absorption spectrum (crossover at 387 nm). This intensity difference is indicative of the Co(II) oxidation state.[47] Additionally, a temperature dependence was observed in the MCD spectrum of Co(II) hCBS over the range 4−25 K. A low-spin Co(II) porphyrin ($S = 1/2$) would be expected to show a temperature-dependent MCD signature. Magnetic saturation curves, which are sensitive to the spin state on the metal, reveal that the *C* term that dominates the MCD spectrum of Co(II) hCBS is an admixture of low-spin, Co(II) ($S = 1/2$) and low-spin, Co (III) ($S = 0$) after subtraction of the native, Fe(III) signal (data not shown). When the MCD spectrum of Co(II)PPIX(1-MeIm) was recorded over a range of temperatures (4−25 K, Supporting Information, Figure S2), a similar temperature dependence for the dominant *C* term was observed, consistent with an $S = 1/2$ spin state on the Co(II) center.

The spin-state and geometry of Co(II) hCBS and of the Co(II)PPIX(1-MeIm) model complex are confirmed by EPR spectroscopy. The low-temperature (4.5 K) X-band EPR spectrum of Co(II)PPIX(1-MeIm) displays axial symmetry with $g_\perp$ = 2.30 and $g_\parallel$ = 2.03 (Supporting Information, Figure S3). This observation further confirms the oxidation state; additionally, the presence and values of the both hyperfine coupling ($A_\parallel^{Co} \sim$ 77G) and superhyperfine coupling ($A_\parallel^{N} \sim$ 17G) are further evidence for the presence of a nitrogenous Lewis base ligated to a 5-coordinate, square-pyramidal Co(II) center with one unpaired electron in the $3d_{z^2}$ orbital. These coupling constants fall squarely

dx.doi.org/10.1021/ic102586b |*Inorg. Chem.* 2011, 50, 4417–4427

Table 4. Comparison of MCD Peak, Crossover, and Trough Positions (nm) between Co(II) hCBS and Fe(II) hCBS[32]

	band	peak	crossover	trough
Co(II) hCBS	Soret (γ)	373	387	400
	α/β	546	554	559
Fe(II) hCBS	Soret (γ)	445	448	452
	α/β	563	566	569

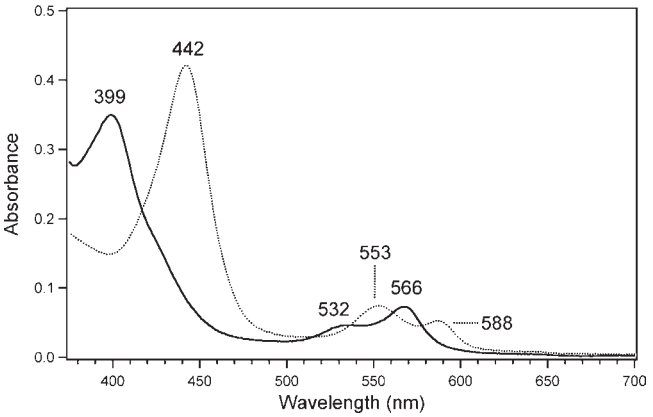

Figure 6. Comparison of electronic absorption spectra of Co−NO hCBS adduct (—) with Co(III) hCBS (····). Each species was 3.9 μM in concentration in a 500 mM CHES buffer and 100 mM NaCl at pH 9.0 and room temperature. After three additions of 100 μL samples of $NO_{(g)}$ to the cuvette headspace, reduction of Co(III) hCBS was achieved by the addition of a stock solution of DTT (~30 mM, 10 μL) to a final concentration of ~1 mM.

in the range of commonly accepted coupling constants for Co(II) porphyrin-containing models and proteins bearing one nitrogenous Lewis base in the axial position.[43,51] Co(II) hCBS displays a similar axially symmetric EPR signal with $g_{\perp}$ = 2.30 (Supporting Information, Figure S4); however, due to problems with protein aggregation at the concentrations necessary for EPR spectroscopy, no hyperfine or superhyperfine coupling could be distinguished to discern any fine structure information. Taken all together, the similarity of the band shapes and positions of the Co(II)PPIX(1-MeIm) spectra to the Co(II) hCBS spectra corroborate the assignment that Co(II) hCBS is five-coordinate and most plausibly retains a single histidine ligand.

Co(II) hCBS Binds NO but Not CO. Like other Co(II)-substituted heme proteins, Co(II) hCBS will bind exogenous $NO_{(g)}$.[53,54] When a limited amount of NO gas is added to prereduced Co(II) hCBS, a new species forms with characteristic absorption bands at 399 nm (Soret), 532 nm (β), and 566 nm (α). The peak positions agree well with previous assignments for 5-coordinate Co-NO adducts.[53,54] Over time, the NO ligand is lost and the spectrum reverts to that of Co(II) hCBS. The Co−NO hCBS adduct may be stabilized by reducing Co(III) hCBS under an atmosphere (i.e., an excess) of NO. The electronic absorption spectrum of the NO adduct thus formed is shown in Figure 6. Co hCBS forms a 5-coordinate NO adduct; this behavior is similar to that of the native Fe hCBS, which forms a 5-coordinate Fe−NO adduct with a loss of both protein-derived axial ligands.[25] Neither the Co(III) nor the Co(II) forms of hCBS bind exogenous $CO_{(g)}$. This behavior is not unusual for Co porphyrin-containing proteins,[50,52] but it is in stark contrast

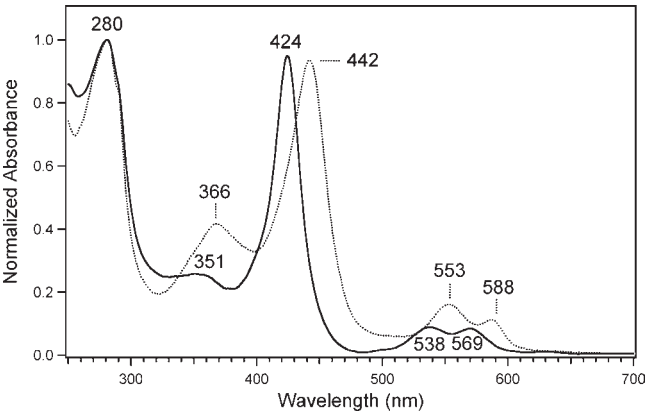

Figure 7. Reoxidized Co(III) hCBS electronic absorption spectrum (—), compared to as-isolated Co(III) hCBS electronic absorption spectrum (····). Each species was 3.9 μM in concentration in a 500 mM CHES buffer and 100 mM NaCl at pH 9.0 and room temperature.

Scheme 1. Depiction of the Coordination States of Co hCBS[a]

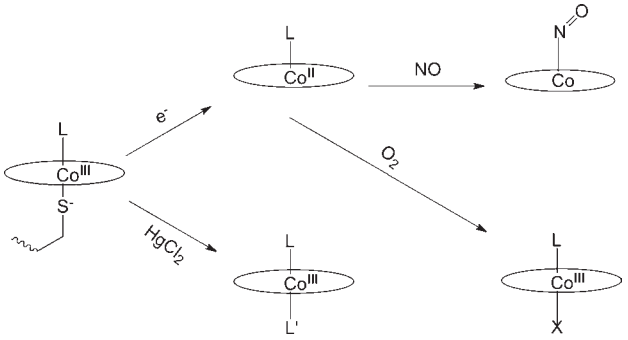

[a] L represents any generic, neutral ligand. X may represent O_2^-, RSO_x—a product of cysteine oxidation—or another generic ligand.

to the native Fe hCBS which binds exogenous $CO_{(g)}$ in the Fe(II) form.[25,55]

Co(II) hCBS Autoxidizes to Co(III) $hCBS_{Reox}$, a Unique Species without a Thiolate Ligand. When Co(II) hCBS is exposed to ambient air, a slow reaction occurs to yield a new Co(III) species that does not bear a thiolate ligand. At room temperature, air was introduced into Co(II) hCBS, and the sample was mixed to distribute oxygen through the solution. Over the course of 48 h, the spectrum converted to that of a new species with peak maxima at 424 nm (Soret), 538 nm (β), and 569 nm (α), as shown in Figure 7. The slow reaction of Co(II) hCBS to give the new species is quite similar to the autoxidation observed as Fe(II) hCBS converts to Fe(III) hCBS upon exposure to the air.[35] However, Co(II) hCBS does not reoxidize to give Co(III) hCBS. The most noticeable difference between Co(III) hCBS and Co(III) hCBS-424_{Reox} is the absence of spectral signatures that are characteristic of thiolate ligation (*vide supra*, compare Figure 2 to Figure 7). Thus, the native thiolate ligation Co(III) hCBS is not restored upon air oxidation. The coordination environment of reoxidized Co(III) $hCBS_{Reox}$ is unclear; the peak positions most closely resemble either a Co(III) porphyrin with two neutral donors or a Co(III)-superoxide adduct with one neutral donor and one superoxide anion as

dx.doi.org/10.1021/ic102586b |*Inorg. Chem.* 2011, 50, 4417–4427

Scheme 2. Reactions Catalyzed by CBS

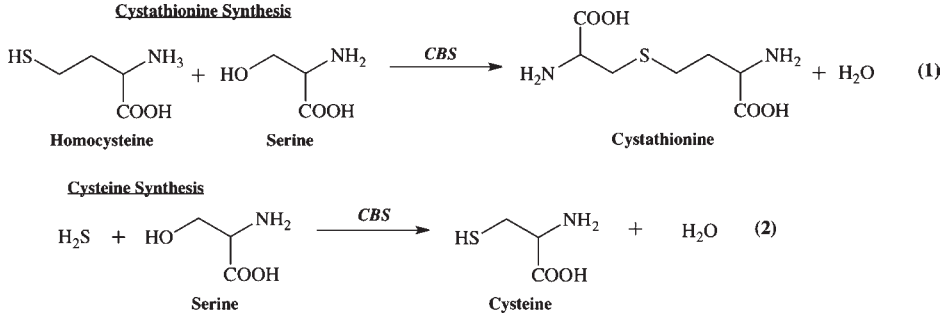

the ligands (Table 1). The fact that Co(III) $hCBS_{Reox}$ does not show identical spectral positions to those of the $HgCl_2$-reacted Co(III) hCBS might plausibly suggest that Co(III) $hCBS_{Reox}$ may be a superoxide adduct; however, binding of an oxidized form of cysteine (cysteic acid) to the reoxidized Co(III) porphyrin cannot be ruled out.[56] A summary of the coordination states of the Co porphyrin in Co hCBS is given in Scheme 1.

Co hCBS Is Maximally Active and AdoMet Responsive Only in the Co(III) State. We compared the activity of Co hCBS in its various coordination and oxidation states, using both the canonical reaction and an alternative CBS reaction (Scheme 2). The alternative reaction tested was the condensation of hydrogen sulfide and serine to produce cysteine and water (**2**). CBS enzymes from *T. cruzi* and *S. cerevisiae* are known to catalyze this cysteine synthesis reaction.[19,57,58] Three states of Co hCBS were tested in each reaction: Co(III) hCBS, Hg-reacted Co(III) hCBS, and Co(II) hCBS; the results are summarized in Table 5. The activity of Co(III) hCBS in the canonical CBS reaction—condensation of homocysteine with serine to form cystathionine (**1**)—was essentially unchanged from that of WT Fe(III) hCBS (Table 5).[29,30] As isolated Co(III) hCBS, with its Cys/His ligation motif, has comparable activity to WT Fe(III) hCBS in the canonical reaction (**1**)[29,30] and ~76% of the activity of WT Fe(III) hCBS for the alternative reaction (**2**). Co(III) hCBS was responsive to AdoMet stimulation in both reactions, with a comparable increase in activity to that observed for Fe(III) hCBS. Thus, the presence of cobalt in the porphyrin does not substantively affect the enzyme activity. Upon disruption of the Co(III)−Cys bond, by reaction of Co(III) hCBS with $HgCl_2$ to form a Co(III) species with two neutral donors (i.e., no cysteine(thiolate)), activity is diminished, but not eliminated, in each reaction. Hg-reacted Co(III) hCBS retains significant activity in the canonical reaction but does not respond to AdoMet stimulation. This enzyme exhibits very modest activity in the alternative reaction. Comparatively, Hg-reacted WT Fe(III) hCBS (which bears a high-spin, 5-coordinate Fe(III) heme without a cysteine(thiolate)[27]) has minimal activity and is unresponsive to AdoMet. A similar diminution of activity with a loss of AdoMet response is seen for Co(II) hCBS, which bears a 5-coordinate Co(II) porphyrin that does not retain its cysteine(thiolate) ligand. It must be noted that some fraction of the residual activity in Co(II) hCBS is due to the small amount (~8%) of Fe(III) hCBS still present, as DTT is unable to reduce WT Fe(III) hCBS to Fe(II) hCBS. Taken together, these results suggest that the native ligation motif (Cys/His) is essential to maintain maximal activity and AdoMet responsiveness for Co hCBS, as is true for Fe hCBS.

Table 5. Comparison of the Enzyme Activities of Co(III) hCBS, Fe(III) hCBS, Hg-Reacted Co(III) hCBS, Hg-Reacted Fe(III) hCBS, and Co(II) hCBS

	specific activity (U)[a,b]	
	cystathionine synthesis (**1**)	cysteine synthesis (**2**)
Fe(III) hCBS	404 ± 25[c]	108 ± 1
Hg-reacted Fe(III) hCBS	19 ± 4	0.8 ± 0.20
Co(III) hCBS	372 ± 19[c]	82 ± 3
Hg-reacted Co(III) hCBS	166 ± 3	7 ± 1
Co(II) hCBS	10 ± 1	10 ± 0.1

[a] 1 unit (U) = μmol product·mg·enzyme^{-1}·hr^{-1}. [b] Values are all reported in the presence of AdoMet and excess PLP. Hg-reacted Fe(III) and Co(III) hCBS as well as Co(II) hCBS were not stimulated by AdoMet. [c] From ref 29.

DISCUSSION

Replacement of heme with other metalloporphyrins has been a useful tool for studying functions and properties of proteins ranging from hemoglobin and myoglobin to cytochrome $P450_{cam}$ and soluble guanylyl cyclase.[43,50,51,53] This tool was applied to investigate the role of heme in the proper folding and expression of CBS.[59] When CBS is expressed in a heme biosynthesis-deficient yeast strain, the protein does not accumulate. CBS expression is rescued by the addition of a chemical chaperone, or by protoporphyrin IX and its metalated derivatives. Modest yields of active Mn hCBS and Co hCBS proteins could be isolated by expression in anaerobically grown heme deficient *E. coli* cells.[59] Recently, we developed an aerobic expression method that enables the isolation of large quantities of high purity Co hCBS sufficient for spectroscopic study.[29,30] This Co hCBS is of particular interest because it is virtually indistinguishable from WT Fe hCBS in terms of its native conformation, enzyme activity, AdoMet responsiveness, PLP saturation, and ability to process alternative substrates.[29,30] These prior expression results implicated a structural role for the CBS heme; the availability of large quantities of Co hCBS enables us to identify the similarities and differences between the Co and Fe coordination environments that may contribute to the structural significance of the heme in CBS. To date, there is still no definitive consensus on heme's function in CBS; this puzzle was the impetus for characterization of the various redox and ligation states of the Co-substituted variant of hCBS (Scheme 1).

dx.doi.org/10.1021/ic102586b |*Inorg. Chem.* 2011, 50, 4417–4427

The spectral features of Co(III) hCBS suggest that the cobalt retains the same coordination environment (Cys/neutral donor, presumably His) as iron in WT Fe(III) hCBS (Cys/His).[10] The similarities between Co(III) hCBS and Fe(III) hCBS highlight the structural importance of the metal−cysteine(thiolate) bond in the function of the CBS heme. First, thiolate coordination to the metal center of the porphyrin in CBS is robust and not metal-specific. That is, thiolate coordination persists when cobalt is substituted in lieu of iron, and the enzyme does not distinguish between the two metals. This identical coordination environment manifests itself spectroscopically and allows for high AdoMet responsive enzymatic activity (both canonical and alternative) even in the presence of Co(III) PPIX (Table 5). In contrast, Hg-reacted Fe(III) and Hg-reacted Co(III) and Co(II) hCBS, which do not bear the thiolate ligand, exhibited impaired activities and are nonresponsive to AdoMet. From these data, it is evident that a metal−thiolate bond is essential for normal CBS function, but the metal does not have to be iron. Furthermore, the slow rate and the odd pH dependence of Co(III) reduction to form Co(II) hCBS suggest a complex process that ultimately results in a loss of the cysteine(thiolate) ligand. Previously, heme in CBS was postulated to function as a redox regulator;[60] however, the behavior of Fe(II) hCBS is incompatible with a redox regulatory process.[23] Fe(II) hCBS is unstable and undergoes a slow loss of activity due to replacement of the cysteine(thiolate) ligand by an unidentified neutral donor ligands.[23] The behavior of Co hCBS, with its very slow reduction, concomitant loss of the thiolate ligand, and minimal activity in the Co(II) state, is similarly incompatible with redox regulation.

A second implication is that the substitution of Co for Fe likely does not disturb the secondary coordination sphere of the porphyrin in CBS. Earlier work has shown that electrostatic interaction of Arg^{266} with the axial ligand Cys^{52} in the WT Fe(III) hCBS is integral to maintaining maximal activity.[49] The proposal was made that changes in the heme coordination environment, in particular at Cys^{52}, may be transmitted through the enzyme to the active site PLP cofactor ~20 Å away. The fact that Co(III) hCBS is fully active suggests that this essential secondary coordination sphere is intact. Without this essential electrostatic interaction, the activity of Hg-reacted Co(III) and Co(II) hCBS is substantially altered. Furthermore, the identical coordination environment and unaffected activity of Co(III) hCBS seems incompatible with the possibilities that the Co porphyrin is bound in a different location in the polypeptide chain or that the enzyme itself is folded improperly. These results suggest that there is a specific structure required for activity, which is defined by the presence of the metalloporphyrin and the specific ligands that are bound.

That the N-terminal heme helps to define the structure of CBS is supported by a variety of evidence. An N-terminal deletion variant lacking heme exhibited low enzymatic activity (~20% of WT);[7] however, the origin of the low activity was not explored. The activity defect may be due to the absence of heme, misfolding, or both. The absence of heme in lower eukaryotic CBS proteins and mechanistic studies of hCBS clearly eliminate any role for heme in catalysis.[17−19] Furthermore, when hCBS is expressed in heme deficient cells, minimal activity is observed. Modest activity restoration is obtained when Fe-, Mn-, Co-, Sn- and ZnPPIX or metal free PPIX are added to the growth medium. Near complete restoration of activity is observed when the chemical chaperone, trimethylamine N-oxide, is added.[59] These observations suggest that proper folding of the enzyme during expression is essential, but that the correctly folded structure may be obtained in a variety of ways. Once properly folded around FePPIX, subsequent disruption of the iron-cysteine(thiolate) ligand bond causes a loss of enzyme activity, which is presumed to result from a change in structure.[16,22,23,25,27] These data, when combined with the fact that hCBS does not discriminate between Fe and Co, together support a structural role of the heme in CBS; perturbation of metal identity in the metalloporphyrin appears not to modify enzyme activity so long as the enzyme is folded correctly and/or the proper metal ligands are maintained.

CONCLUSION

In this study, we demonstrated that cobalt-substituted cystathionine β-synthase contains a novel Cys/His cobalt(III) porphyrin coordination environment, which is unprecedented among cobalt-substituted hemeproteins. Co(III) hCBS is fully active and robustly maintains the native ligation motif that is essential for enzymatic activity. Co(III) hCBS may be reduced to Co(II) hCBS, which bears a 5-coordinate Co(II) porphyrin without the cysteine(thiolate) and shows reduced enzymatic activity. Unsurprisingly, this Co(II) state will bind $NO_{(g)}$ but not $CO_{(g)}$. Co(II) hCBS may be reoxidized to a different Co(III) form (Co(III) $hCBS_{Reox}$), in which the cysteine(thiolate) ligation is not restored. When considered in light of the functional activity of both Co hCBS and Fe hCBS, these findings are consistent with the hypothesis that the heme in cystathionine β-synthase plays a structural role.

ASSOCIATED CONTENT

Supporting Information. Figures showing electronic absorption and MCD spectra of Co(III)PPIX(1-MeIm)$_2$ (S1), electronic absorption and MCD spectra of Co(II)PPIX(1-MeIm) (S2), the X-band EPR spectrum of Co(II)PPIX(1-MeIm) including its best fit simulation (S3), and the X-band EPR spectrum of Co(II) hCBS (S4). This material is available free of charge via the Internet at http://pubs.acs.org.

AUTHOR INFORMATION

Corresponding Author

*Tel.: 608-262-0328. Fax: 608-262-6143. E-mail: burstyn@chem.wisc.edu.

ACKNOWLEDGMENT

The authors of this paper wish to express thanks to Professor Thomas C. Brunold (University of Wisconsin—Madison) and his research group for their expertise, many fruitful discussions, and the generous use of their instrumentation. We also thank Dr. Frank Neese (MPI Mülheim, Mülheim, Germany) for the use of ORCA and the WEPR spectral fitting program. This work was supported by NIH grant HL-065217 to J.P.K and J.N.B, by American Heart Association Grant-in-Aid 09GRNT2110159 to J.P.K, and by Postdoctoral Fellowship 0920079G from the American Heart Association to T.M.

ABBREVIATIONS

hCBS, human cystathionine β-synthase; PLP, pyridoxal-5′-phosphate; AdoMet, S-adenosyl-methionine; PPIX, protoporphyrin IX; Co hCBS, cobalt cystathionine β-synthase; Co

$hCBS_{Reox}$, ambiently reoxidized cobalt cystathionine β-synthase; DTT, dithiothreitol; ImH, imidazole; 1-MeIm, 1-methyl imidazole; 2-MeImH, 2-methyl imidazole; 4-MeImH, 4-methyl imidazole; MCD, magnetic circular dichroism; EPR, electron paramagnetic resonance; CHES, N-cyclohexyl-2-aminoethanesulfonic acid; HEPES, 4-(2-hydroxyethyl)-1-piperazineethanesulfonic acid; MES, 2-(*N*-morpholino)ethanesulfonic acid; ICP-OES, inductively coupled plasma optical emission spectroscopy; LMCT, ligand-to-metal charge transfer transition; TD-DFT, time-dependent density-functional theory; TGE, thioglycolate ethyl ester 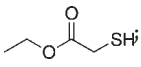 ; TN, thionalide 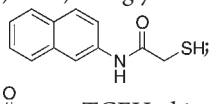 ; TGB, thioglycolate *n*-butyl ester 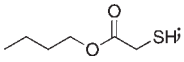 ; TGEH, thioglycolate 2-ethylhexyl ester 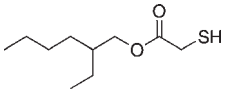

REFERENCES

(1) Mudd, S. H.; Levy, H. L.; Kraus, J. P. *Disorders of transsulfuration*; McGraw-Hill: New York, 2001; p 49.

(2) Clarke, R.; Smith, A. D.; Jobst, K. A.; Refsum, H.; Sutton, L.; Ueland, P. M. *Arch. Neurol.* **1998**, *55*, 1449–1455.

(3) Mattson, M. P.; Shea, T. B. *Trends Neurosci.* **2003**, *26*, 137–146.

(4) Refsum, H.; Ueland, P. M.; Nygard, O.; Vollset, S. E. *Annu. Rev. Med.* **1998**, *49*, 31–62.

(5) Mills, J. L.; McPartlin, J. M.; Kirke, P. N.; Lee, Y. J.; Conley, M. R.; Weir, D. G.; Scott, J. M. *Lancet* **1995**, *345*, 149–151.

(6) Kery, V.; Bukovska, G.; Kraus, J. P. *J. Biol. Chem.* **1994**, *269*, 25283–25288.

(7) Oliveriusová, J.; Kery, V.; Maclean, K. N.; Kraus, J. P. *J. Biol. Chem.* **2002**, *277*, 48386–48394.

(8) Janosik, M.; Kery, V.; Gaustadnes, M.; MacLean, K. N.; Kraus, J. P. *Biochemistry* **2001**, *40*, 10625–10633.

(9) Kery, V.; Poneleit, L.; Kraus, J. P. *Arch. Biochem. Biophys.* **1998**, *355*, 222–232.

(10) Meier, M.; Janosik, M.; Kery, V.; Kraus, J. P.; Burkhard, P. *EMBO J.* **2001**, *20*, 3910–3916.

(11) Taoka, S.; Lepore, B. W.; Kabil, O.; Ojha, S.; Ringe, D.; Banerjee, R. *Biochemistry* **2002**, *41*, 10454–10461.

(12) Ojha, S.; Hwang, J.; Kabil, O.; Penner-Hahn, J. E.; Banerjee, R. *Biochemistry* **2000**, *39*, 10542–10547.

(13) Kery, V.; Poneleit, L.; Meyer, J. D.; Manning, M. C.; Kraus, J. P. *Biochemistry* **1999**, *38*, 2716–2724.

(14) Evande, R.; Ojha, S.; Banerjee, R. *Arch. Biochem. Biophys.* **2004**, *427*, 188–196.

(15) Bruno, S.; Schiaretti, F.; Burkhard, P.; Kraus, J. P.; Janosik, M.; Mozzarelli, A. *J. Biol. Chem.* **2001**, *276*, 16–19.

(16) Taoka, S.; West, M.; Banerjee, R. *Biochemistry* **1999**, *38*, 2738–2744.

(17) Jhee, K.-H.; McPhie, P.; Miles, E. W. *J. Biol. Chem.* **2000**, *275*, 11541–11544.

(18) Maclean, K. N.; Janosk, M.; Oliveriusov, J.; Kery, V.; Kraus, J. P. *J. Inorg. Biochem.* **2000**, *81*, 161–171.

(19) Nozaki, T.; Shigeta, Y.; Saito-Nakano, Y.; Imada, M.; Kruger, W. D. *J. Biol. Chem.* **2001**, *276*, 6516–6523.

(20) Taoka, S.; Ohja, S.; Shan, X.; Kruger, W. D.; Banerjee, R. *J. Biol. Chem.* **1998**, *273*, 25179–25184.

(21) Chen, Z.; Chakraborty, S.; Banerjee, R. *J. Biol. Chem.* **1995**, *270*, 12946–12949.

(22) Cherney, M. M.; Pazicni, S.; Frank, N.; Marvin, K. A.; Kraus, J. P.; Burstyn, J. N. *Biochemistry* **2007**, *46*, 13199–13210.

(23) Pazicni, S.; Cherney, M. M.; Lukat-Rogers, G. S.; Oliveriusová, J.; Rodgers, K. R.; Kraus, J. P.; Burstyn, J. N. *Biochemistry* **2005**, *44*, 16785–16795.

(24) Frank, N.; Kent, J. O.; Meier, M.; Kraus, J. P. *Arch. Biochem. Biophys.* **2008**, *470*, 64–72.

(25) Taoka, S.; Banerjee, R. *J. Inorg. Biochem.* **2001**, *87*, 245–251.

(26) Shintani, T.; Iwabuchi, T.; Soga, T.; Kato, Y.; Yamamoto, T.; Takano, N.; Hishiki, T.; Ueno, Y.; Ikeda, S.; Sakuragawa, T.; Ishikawa, K.; Goda, N.; Kitagawa, Y.; Kajimura, M.; Matsumoto, K.; Suematsu, M. *Hepatology* **2009**, *49*, 141–150.

(27) Taoka, S.; Green, E. L.; Loehr, T. M.; Banerjee, R. *J. Inorg. Biochem.* **2001**, *87*, 253–259.

(28) Celano, L.; Gil, M.; Carballal, S.; Durán, R.; Denicola, A.; Banerjee, R.; Alvarez, B. *Arch. Biochem. Biophys.* **2009**, *491*, 96–105.

(29) Majtan, T.; Freeman, K. M.; Smith, A. T.; Burstyn, J. N.; Kraus, J. P. *Arch. Biochem. Biophys.* **2011**, *508*, 25–30.

(30) Majtan, T.; Frerman, F. E.; Kraus, J. P. *BioMetals* **2011**, *24*, 335–347.

(31) Janosik, M.; Meier, M.; Kery, V.; Oliveriusov, J.; Burkhard, K. A.; Kraus, J. P. *Acta Crystallogr., Sect D: Biol. Crystallogr.* **2001**, *57*, 289–291.

(32) Pazicni, S.; Lukat-Rodgers, G. S.; Oliveriusová, J.; Rees, K. A.; Parks, R. B.; Clark, R. W.; Kraus, J. P.; Rodgers, K. R.; Burstyn, J. N. *Biochemistry* **2004**, *43*, 14684–14695.

(33) Neese, F. *Electronic structure and spectroscopy of novel copper chromophores in biology*; University of Konstanz: Konstanz, Germany, 1997.

(34) Dey, A.; Okamura, T.-A.; Ueyama, N.; Hedman, B.; Hodgson, K. O.; Solomon, E. I. *J. Am. Chem. Soc.* **2005**, *127*, 12046–12053.

(35) Pazicni, S. *Towards Understanding the Role of the Heme Cofactor in Cystathionine β-Synthase*; University of Wisconsin: Madison, WI, 2006.

(36) Neese, F.; Olbrich, G. *Chem. Phys. Lett.* **2002**, *362*, 170–178.

(37) Lee, C.; Yang, W.; Parr, R. G. *Phys. Rev. B: Condens. Matter Mater. Phys.* **1988**, *37*, 785–789.

(38) Laaksonen, L. *J. Mol. Graph.* **1992**, *10*, 33–34.

(39) Bergman, D. L.; Laaksonen, A. *J. Mol. Graphics Modell.* **1997**, *15*, 301–306.

(40) Gaitonde, M. K. *Biochem. J.* **1967**, *104*, 627–633.

(41) Dickinson, L. C.; Chien, J. C. W. *Biochemistry* **1975**, *14*, 3526–3533.

(42) Falk, J. E. *Porphyrins and Metalloporphyrins: Their General, Physical, and Coordination Chemistry, and Laboratory Methods*; Elsevier: Amsterdam, 1964.

(43) Wagner, G. C.; Gunsalus, I. C.; Wang, M. Y.; Hoffman, B. M. *J. Biol. Chem.* **1981**, *256*, 6266–6273.

(44) Johnson, M. K. In *Physical Methods in Bioinorganic Chemistry*; Que, L., Jr., Ed.; University Science Books: Sausalito, CA, 2000; pp 233−285.

(45) Gale, R.; McCaffery, A. J.; Rowe, M. D. *J. Chem. Soc. Dalton* **1972**, 596–604.

(46) Dawson, J. H.; Andersson, L. A.; Sono, M. *J. Biol. Chem.* **1983**, *258*, 13637–13645.

(47) Gasyna, Z.; Stillman, M. J. *Inorg. Chem.* **1990**, *29*, 5101–5109.

(48) Kitanishi, K.; Igarashi, J.; Hayasaka, K.; Hikage, N.; Saiful, I.; Yamauchi, S.; Uchida, T.; Ishimori, K.; Shimizu, T. *Biochemistry* **2008**, *47*, 6157–6168.

(49) Singh, S.; Madzelan, P.; Stasser, J.; Weeks, C. L.; Becker, D.; Spiro, T. G.; Penner-Hahn, J.; Banerjee, R. *J. Inorg. Biochem.* **2009**, *103*, 689–697.

(50) Yonetani, T.; Yamamoto, H.; Woodrow, G. V., III. *J. Biol. Chem.* **1974**, *249*, 682–690.

(51) Yonetani, T.; Yamamoto, H.; Iizuka, T. *J. Biol. Chem.* **1974**, *249*, 2168–2174.

(52) Wang, M. Y.; Hoffman, B. M.; Hollenberg, P. F. *J. Biol. Chem.* **1977**, *252*, 6268–6275.

(53) Dierks, E. A.; Hu, S.; Vogel, K. M.; Yu, A. E.; Spiro, T. G.; Burstyn, J. N. *J. Am. Chem. Soc.* **1997**, *119*, 7316–7323.

(54) Makino, R.; Matsuda, H.; Obayashi, E.; Shiro, Y.; Iizuka, T.; Hori, H. *J. Biol. Chem.* **1999**, *274*, 7714–7723.

(55) Puranik, M.; Weeks, C. L.; Lahaye, D.; Kabil, Ö.; Shinichi, T.; Nielsen, S. B.; Groves, J. T.; Banerjee, R.; Spiro, T. G. *J. Biol. Chem.* **2006**, *281*, 13433–13438.
(56) Choudhury, K.; Sundaramoorthy, M.; Hickman, A.; Yonetani, T.; Woehl, E.; Dunn, M. F.; Puolos, T. L. *J. Biol. Chem.* **1994**, *269*, 20239–20249.
(57) Braunstein, A. E.; Goryachenkova, E. V.; Lac, N. D. *Biochim. Biophys. Acta* **1969**, *171*, 366–368.
(58) Ono, B.-I.; Kijima, K.; Inoue, T.; Miyoshi, S.-I.; Matsuda, A.; Shinoda, S. *Yeast* **1993**, *10*, 333–339.
(59) Majtan, T.; Singh, L. R.; Wang, L.; Kruger, W. D.; Kraus, J. P. *J. Biol. Chem.* **2008**, *283*, 34588–34595.
(60) Banerjee, R.; Zou, C.-G. *Arch. Biochem. Biophys.* **2005**, *433*, 144–156.
(61) Dickinson, L. C.; Chien, J. C. W. *Biochemistry* **1975**, *14*, 3534–3542.
(62) Sakurai, H.; Ishizu, K.; Sugimoto, H.; Gunsalus, I. C. *J. Inorg. Biochem.* **1986**, *26*, 55–62.